VILNIUS TECH
Vilnius Gediminas Technical University

Proceedings of the 13th International Scientific Conference

ENVIRONMENTAL ENGINEERING

April 23–24, 2026, Vilnius, LITHUANIA

eISSN 2029-7092
eISBN 978-609-476-444-8
Article ID: enviro.2026.2307
https://doi.org/10.3846/enviro.2026.2307

THERMAL PERFORMANCE OF A SILICA GEL-WATER VAPOR ADSORPTION SYSTEM AS AN ALTERNATIVE COOLING TECHNOLOGY

Katarzyna KATANA, Adam SZELĄGOWSKI, Andrzej GRZEBIELEC*

Warsaw University of Technology, st. plac Politechniki 1, 00-665 Warsaw, Poland

Received 15 January 2026; revised 28 January 2026; accepted 15 February 2026

Abstract. Adsorption-based cooling is an alternative to conventional vapor-compression systems that have a high environmental impact and account for a significant share of global energy consumption. This study presents an experimental and analytical investigation of a two-bed adsorption cooling system operating with a water/silica-gel working pair. The device consists of a refrigerant circuit (water vapor) and a secondary water circuit that provides supplies or removes heat from the beds when necessary. The refrigerant circuit includes two adsorption beds, a condenser, an expansion valve, and an evaporator. The system operates in alternating half-cycles, with one bed undergoing desorption while the other performs adsorption. Measurements of temperature, pressure, and volumetric flow rates were conducted over nearly three half-cycles. Theoretical cooling capacity was calculated at 6.652 kJ, which corresponds to the EER (Energy Efficiency Ratio) equal to 0.0405. To overcome issues associated with limited thermal contact between the surface of the heat exchanger and the adsorbent particles as well as low thermal conductivity of silica gel, it should be applied directly onto the heat exchanger's surface in the form of coatings instead of the traditional loose packing of adsorbent granules. Additionally, enhancing the system's performance can be achieved by implementing heat and mass recovery. These findings provide insights into the design of adsorption-based refrigeration, emphasizing environmentally friendly and efficient alternatives to conventional vapor-compression systems.

Keywords: adsorption, silica gel, cooling, refrigeration, energy efficiency.

1. Introduction

Refrigeration accounts for approximately 10% of global energy consumption, and for buildings it is responsible for as much as 20% of total energy demand (International Energy Agency, 2018). Given the current state of the climate, there is a clear need to seek innovative, more environmentally sustainable solutions and to optimize existing refrigeration systems.

The most widely used cooling method is vapor-compression refrigeration. Vapor-compression refrigeration systems operate on the principle of transferring heat from a low-temperature environment to a higher-temperature sink. In the evaporator, heat is absorbed by the refrigerant, causing it to undergo a phase change from liquid to vapor at nearly constant pressure. This heat removal from the surroundings produces the desired cooling effect.

A key advantage of vapor-compression systems is their relatively high cooling efficiency, commonly expressed by the Energy Efficiency Ratio (EER). The EER represents the amount of cooling delivered per unit of electrical energy consumed, primarily by the compressor, but also by fans and other auxiliary components. Typical EER values range from 1 to 5, depending on system design, operating conditions, and the thermodynamic properties of the refrigerant. Currently, the most used refrigerants in the European Union include R134a, R32, R125, R152a and mixtures such as R410A, R404A and R407C (Ludig et al., 2024). All these refrigerants belong to the group of hydrofluorocarbons (HFCs). Figure 1 illustrates the total quantity of fluorinated gases supplied to the EU market over the past decade, broken down into HFCs, PFCs and SF_6. The data show a clear downward trend in the supply of HFCs, reflecting the impact of the EU F-gas Regulation and the phasedown schedule. Figure 2 presents the same data converted into CO_2-equivalent values, highlighting the climate impact of each gas group. Despite the relatively small volumes of PFCs and SF_6, their high Global Warming Potentials (GWPs) make them significant contributors to total CO_2-equivalent emissions. The overall decline in emissions shown in Figure 2 further demonstrates the effectiveness of regulatory measures aimed at reducing the environmental footprint of fluorinated gases.

* Corresponding author. E-mail: *andrzej.grzebielec@pw.edu.pl*

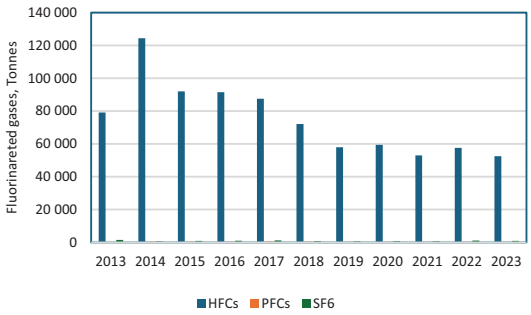

Figure 1. Total EU supply of fluorinated gases (Ludig et al., 2024)

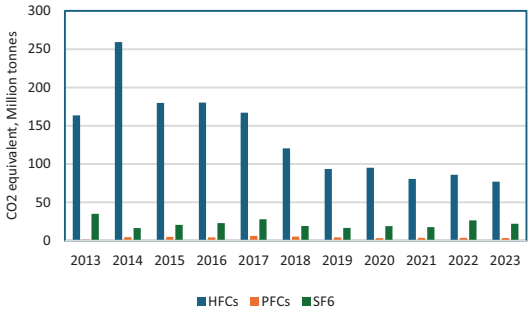

Figure 2. Total EU supply of fluorinated gases (CO2e) (Ludig et al., 2024)

The use of these substances significantly contributes to the intensification of the greenhouse effect, which is expressed through the Global Warming Potential (GWP) index (Australian Government, 2024). GWP represents the warming impact of 1 kg of a given gas over a 100-year period relative to 1 kg of CO_2, for which GWP = 1. For the most common HFC refrigerants, the GWP values are approximately 2088 (R410A), 1430 (R134a), and 675 (R32) (The European Parliament & The Council of the European Union, 2024; Darby, 2014). These high GWP values explain why, despite the decreasing mass of HFCs shown in Figures 1–2, their CO_2-equivalent impact remains substantial and remains a key target of regulatory measures in the EU.

Other popular refrigerant, without fluoride, such as R717 (ammonia, GWP = 0), R290 (propane, GWP = 0.02), or R744 (carbon dioxide, GWP = 1.0), are characterized by negligible or zero GWP values. However, their use involves various challenges that often limit their application. Ammonia, for example, is toxic, flammable and exhibits low material compatibility (incompatibility with copper) which significantly restricts its use, particularly in smaller units or facilities occupied by people. Propane belongs to the A3 safety category (highly flammable refrigerants) and is therefore commonly used in small-scale devices due to requirements related to minimum enclosed room volume and ventilation. Carbon dioxide has exceptionally low critical parameters (73.6 bar and 31.1 °C), which necessitates the use of transcritical systems that do not utilize latent heat due to lack of condensation in the upper heat exchanger – gas cooler (Baheta et al., 2015). It also requires use of components that are resistant to high pressures up to 120–130 bar. Considering increasingly stringent regulations of environmentally harmful or hazardous refrigerants, refrigeration systems that operate without substances, which require special considerations, or significantly limit their use provide environmental benefits, enhance operational safety, and ensure greater regulatory flexibility.

Due to the limitations associated with the use of working fluids in conventional vapor-compression refrigeration systems, various alternative cooling technologies are being actively developed. Among the most promising solutions are (Grzebielec, 2024):

- sorption cooling systems (absorption, adsorption);
- thermoelectric systems;
- systems based on the magnetocaloric effect;
- systems based on the elastocaloric effect;
- systems utilizing the reversed Stirling cycle;
- thermoacoustic cooling systems;
- ejector refrigeration systems.

In many of these alternative technologies, the achievable cooling capacity is limited by the physical principles and design constraints of the devices, which means that most of them can only be implemented at scales of up to several tens of kilowatts. Only sorption and ejector systems can be constructed across a wide range of capacities-from a few watts to several megawatts (Grzebielec, 2024; Sahu et al., 2026).

Absorption, adsorption, and ejector refrigeration systems are driven by heat. Consequently, they represent technologies capable of utilizing thermal energy from solar collectors or industrial waste heat. Absorption systems are already well established on the market, most commonly using water-ammonia or lithium bromide-water working pairs. Ejector systems, on the other hand, operate with conventional refrigerants, which means they are subject to similar legislative restrictions as vapor-compression installations (Butrymowicz et al., 2014).

For this reason, the authors of this study decided to focus on adsorption-based refrigeration systems, which, compared to absorption systems – can operate at significantly lower driving temperatures. This characteristic gives them broader implementation potential across various industrial applications where low-grade waste heat is readily available.

2. Methodology

Silica gel is a type of desiccant made from silicon dioxide (SiO_2); it occurs naturally in sand and quartz. It is non-toxic, widely available, relatively inexpensive, and capable of adsorbing large amounts of water vapor at low pressures (on the order of 0.2–0.4 g H_2O per g of silica gel), which makes it attractive for applications in thermal energy storage and adsorption cooling devices

as shown in Figure 3. Silica gel can achieve up to 95% regeneration using a heat source with a temperature of 90 °C (Hanif et al., 2023).

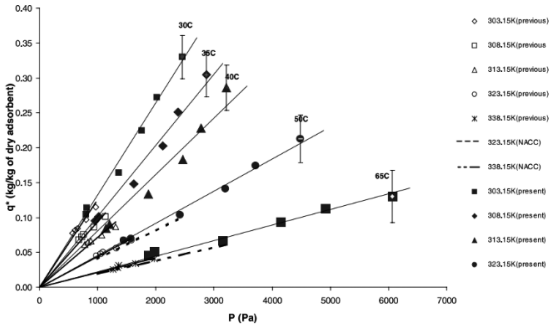

Figure 3. Isotherm data for the Type 3A silica gel-water system (Hanif et al., 2023)

Another advantage of adsorption cooling devices is their lack of moving parts, most notably a compressor, which reduces the failure frequency, electrical energy consumption and noise levels. Additionally, the usage of naturally occurring, zero-emissions substances is aligned with the goal of developing environmentally sustainable solutions. It is possible to achieve relatively high COP levels in adsorption chillers with a silica gel and water pair such as 0.4 or even 0.62 if using solar power (Najeh et al., 2016).

This study concludes an analysis of a two-bed adsorption cooling system using silica-gel and water as a working pair shown in Figure 4.

Figure 4. Silica gel-water vapor adsorption system

The device consists of two circuits, the refrigerant circuit and the water circuit. The refrigerant circuit includes two beds, A1 and A2, four ball valves (V1, V2, V3, V4), a condenser, an expansion valve and an evaporator. The system diagram is shown in Figure 5.

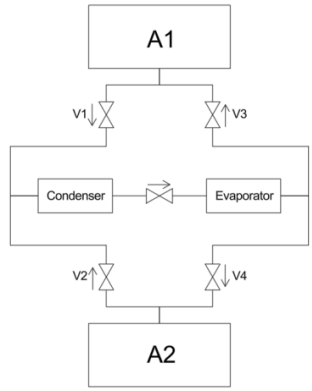

Figure 5. Refrigerant circuit

The cycle consists of two half-cycles. In the first half-cycle, heat is supplied to bed A2 causing working fluid the working fluid to desorb as water vapor. The gas passes through valve V2, enters the condenser, and releases heat to the surroundings, condensing in the process. The refrigerant then expands through the expansion valve and enters the evaporator, where it absorbs heat from the environment during a phase change. The vapor leaving the evaporator passes through valve V3 and enters bed A1, where it is adsorbed. In the next phase, the roles of the beds are reversed: heat is supplied to bed A1, which undergoes desorption, while heat is removed from bed A2, thus the system returns to its initial state, and the device is ready to start the next cycle.

During the desorption process, heat is supplied to the bed, while during adsorption, heat is extracted. This heat transfer is accomplished via a secondary water loop. Both beds (A1 and A2) are equipped with integrated heat exchangers, enabling the delivery and removal of heat during the respective half-cycles.

3. Results and calculations

The experimental setup described in a previous chapter was instrumented as follows: temperature measurements were performed using class A PT100 resistance temperature sensors (RTDs), pressure was measured with class A PC-28 pressure transducers, and the volumetric flow rate was determined using vortex-type flow meters. An analysis covers nearly 3 half-cycles. During the operation of the adsorption unit, the following variables were recorded:

t [s] – time;
$p(A1)$ [kPa] – pressure in A1 bed;
$p(A1)$ [kPa] – pressure in A2 bed;
$t_1(A1)$ [°C] – inlet A1 temperature;
$t_2(A1)$ [°C] – outlet A1 temperature;
$t_3(A2)$ [°C] – inlet A2 temperature;
$t_4(A2)$ [°C] – outlet A2 temperature;
$\dot{\upsilon}_{heating}$ [l/min] – volumetric flow rate in the heating loop;
$\dot{\upsilon}_{cooling}$ [l/min] – volumetric flow rate in the cooling loop.

The absolute pressures in beds A1 and A2 during almost 3 half-cycles are presented in Figure 6. Each half-cycle ended when the pressures stabilized and the difference between the inlet and outlet temperature of beds approached zero. Duration of the first half-cycle was approximately 195 min. Pressure inside the A2 bed rises to 23.7 kP(a) during the process of desorption, while the absolute pressure inside bed A1 is maintained at a 1.4–1.7 kPa(a) level. In the next half-cycle, roles of the beds are reversed, thus the pressure profiles are as well.

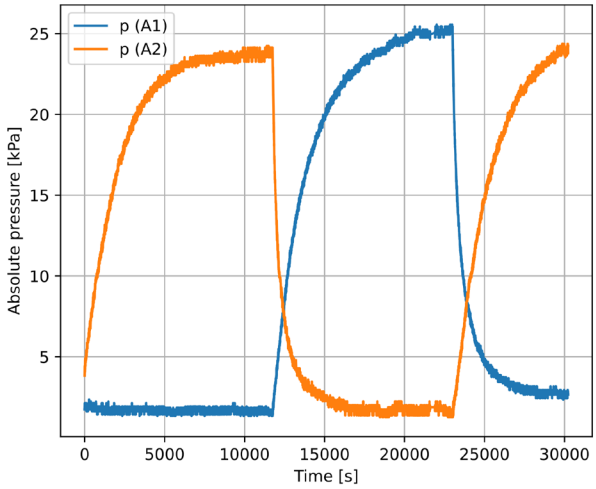

Figure 6. Absolute pressures in A1 and A2 beds

The inlet and outlet temperatures of the heat exchangers installed in beds A1 and A2 are shown as a function of time in Figure 7. The temperature of the supplied heat, i.e., the water flowing through a heat exchanger is approximately 75 °C, whereas the cooling temperature is 20 °C. A rise in the cooling water temperature throughout the half-cycles up to 25 °C is a result of water temperature increase in a water buffer tank.

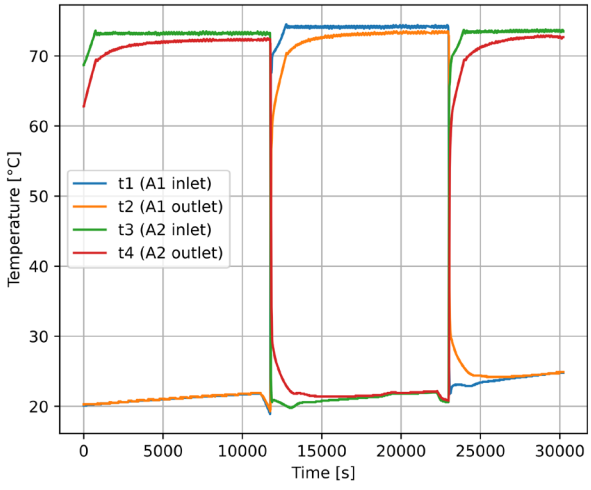

Figure 7. A1 and A2 heat exchanger's inlet and outlet temperatures

Figure 8 shows volumetric flow rates of cooling and heating mediums in a secondary water loop. Mean volumetric flow of the cooling medium is equal to 1.48 l/min, while for heating medium it is equal to 1.38 l/min.

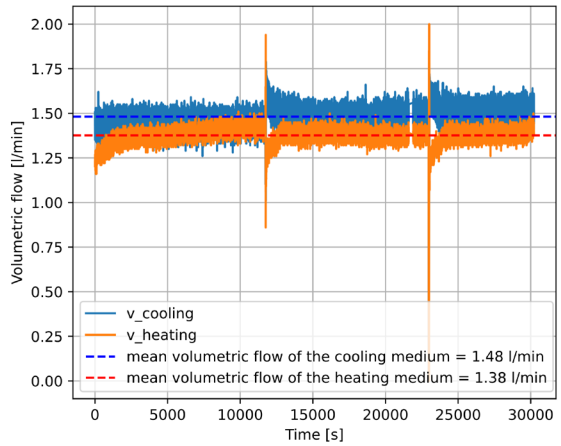

Figure 8. Volumetric flowrate of cooling and heating water in a secondary loop

When the heat is removed from the A1 bed during the adsorption process and applied to the A2 bed during the desorption process (first half-cycle), the heat flow calculations use $\dot{\upsilon}_{cooling}$ for A1 and $\dot{\upsilon}_{heating}$ for A2. When the roles are reversed i.e., A1 is heated (desorption) and A2 is cooled (adsorption), $\dot{\upsilon}_{heating}$ is used for A1 and $\dot{\upsilon}_{cooling}$ is used for A2 (second half-cycle).

The heat flow supplied to or removed from the beds was calculated using the temperature difference of water at the inlet and outlet of the heat exchangers installed in beds A1 and A2, together with the water volumetric flow rate.

$$\dot{Q} = (t_1 - t_2) \times c_p \times \rho \times \dot{v}_i, \tag{1}$$

where ρ and c_p are respectively the water density and specific heat capacity.

The heat flows are shown in Figure 9. Positive values correspond to heat supplied to each bed, whereas negative values indicate removed heat.

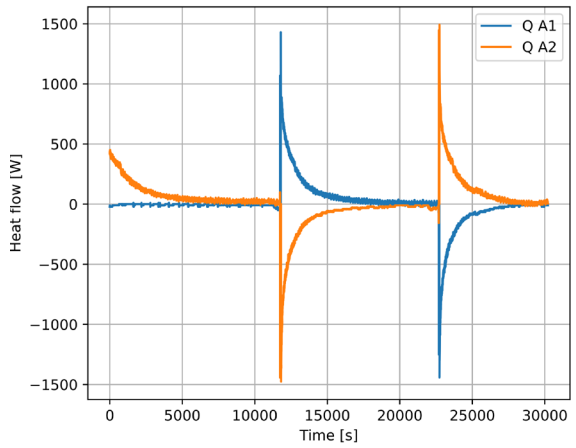

Figure 9. Heat flows to and from A1 and A2 beds

The total energy supplied and removed was obtained by multiplying each measurement by the 1 s time step and summing over all steps. Amounts of heat removed and supplied to A1 and A2 beds are presented in Table 1.

Table 1. Amounts of heat supplied and removed from A1 and A2 beds

Heat transfer, kJ	
First half-cycle	
A1 bed (adsorption)	–32.274
A2 bed (desorption)	840.032
Second half-cycle	
A1 bed (desorption)	959.969
A2 bed (adsorption)	–985.06
Third half-cycle	
A1 bed (adsorption)	–767.303
A2 bed (desorption)	868.604

Low value of removed heat from A1 bed during the first half cycle means that that bed was initially in a cooled state at the beginning of the operation The differences between supplied and removed heat result from heat losses to the surroundings.

The amounts of adsorbed and desorbed water vapor were calculated based on the pressure values in the beds, the mass of the working fluid (water vapor) present in the gas phase within the bed was determined. At such low pressures, water vapor can be reasonably treated as an ideal gas, therefore the masses of water at the start of each half-cycle were determined using the Clapeyron equation:

$$m = \frac{p \times V_{free}}{R \times T}, \tag{2}$$

where, $R = 461.5\ \mathrm{kJ/kg \cdot K}$ is water vapor gas constant, $V_{free} = 0.02\ \mathrm{m^3}$ is the free volume in each bed, which also includes the bulk density of the silica gel, p (pressure) and T (absolute temperature) were measured.

Table 2. Amounts of adsorbed and desorbed water vapor over each half cycle.

Water vapor mass, g	
First half-cycle	
A1 bed (adsorption)	0.044
A2 bed (desorption)	2.546
Second half-cycle	
A1 bed (desorption)	3.068
A2 bed (adsorption)	2.898
Third half-cycle	
A1 bed (adsorption)	2.879
A2 bed (desorption)	2.946

By evaluating the water vapor masses at the start of each half-cycle, the amounts of adsorbed and desorbed water vapor over the half-cycle were determined and are presented in Table 2.

4. Analysis

Based on the obtained results and the device described in Section 2, the theoretical cooling capacity was evaluated. A condensation pressure corresponding to a temperature of 35 °C and an evaporation pressure of 1.5 kPa were assumed. The specific enthalpies at these two states – at the end of condensation (i.e., at the beginning of evaporation) and at the end of evaporation were determined and are equal to:

$$h_{vapor}(p = 1.5\ \mathrm{kPa}) = 2524.721\ \mathrm{kJ/kg}; \tag{3}$$

$$h_{liquid}(t = 35\ ^{\circ}\mathrm{C}) = 147.007\ \mathrm{kJ/kg}. \tag{4}$$

The cooling capacity is calculated using the following equation:

$$Q_{cool} = (h_{vapor} - h_{vapliquid}) \times \Delta m_{des}. \tag{5}$$

The average cooling capacity and heat supplied for each is equal to:

$$Q = 6.787\ \mathrm{kJ}; \tag{6}$$

$$Q_{supplied} = 889.535\ \mathrm{kJ}. \tag{7}$$

Therefore, the estimated EER (Energy Efficiency Ratio) of the system is equal to:

$$EER = \frac{Q_{cool}}{Q_{supplied}} = 0.00763. \tag{8}$$

In practical applications, this low efficiency can be offset if the system is powered by waste heat sources or renewable energy sources such as solar energy.

5. Future work

Enhancing the system's performance can be achieved by implementing heat and mass recovery. Mass recovery involves adding an additional bypass with a valve between two beds, which enables pressure equalization between an adsorbed (low pressure) and desorbed bed (high pressure) at the end of the half-cycle. Water vapor in the high-pressure bed is transferred to a low-pressure bed because of pressure difference. This allows for more refrigerant (water vapor) to pass through the refrigerant circuit, including the evaporator, which consequently increases the system's cooling power, since the water vapor already present above the bed does not have to be re-adsorbed during the adsorption process in that bed. Additionally, required adsorption and desorption pressure levels are reached quicker, which shortens the cycle's duration. On the other hand, heat recovery utilizes heat that must be removed from bed after desorption. It is partially transferred to the other bed, thereby reducing

the total external heat required. Studies show that implementing mass recovery can increase the COP levels by 18,3% whereas heat recovery shows a 34,4% COP increase (Liu et al., 2005).

Despite the advantages of the silica gel described in first chapter, the practical use presents significant technical challenges such as limited thermal contact between the surface of the heat exchanger and the adsorbent particles. Heat must pass not only through the void spaces between the granules but also through the bulk of each particle, which significantly reduces the rate and efficiency of heat transfer (Grzebielec & Szelągowski, 2020). Another important limitation is the very low thermal conductivity of silica gel, which is only about 0.1–0.2 W/(m·K) (Grzebielec, 2018). This means that even if heat reaches the outer surface of a granule, its distribution throughout the entire particle volume is slow. In practice, this means that a large fraction of the adsorbent may remain "unused," because heat does not penetrate its interior within a sufficiently short time. This leads to a smaller amount of recovered water vapor and lower storage efficiency. Similarly, in adsorption cooling devices, inefficient heat transfer results in slower adsorption-desorption cycles, which limits the cooling capacity of the system and increases its response time to changing thermal loads (Thu et al., 2013).

A possible solution to these challenges is to use crushed silica gel in the form of coatings applied directly onto the heat exchanger surface instead of the traditional loose packing of adsorbent granules. This approach allows for:

- increasing the thermal contact area between the heat exchanger and the adsorbent,
- reducing the heat conduction path within the material,
- increasing the effective participation of the adsorbent mass in the desorption and adsorption processes.

To obtain durable and efficient adsorption coatings, silica gel could be mixed with an adhesive material and then applied uniformly onto the heat exchanger surface and subsequently cured thermally, ensuring good adhesion and stability of the coating.

The effect of silica gel particle size on adsorption capacity has been investigated (Szelągowski & Chwieduk, 2025). Three silica gel fractions were mixed with an adhesive water-based acrylic solution. Smallest fraction < 0.4 mm exhibited the lowest adsorption capacity compared to fractions up to 1 mm diameter, which may suggest that using too fine silica gel particles negatively affects the effectiveness of sorption processes.

6. Conclusions

Adsorption cooling cycles offer an environmentally sustainable alternative to conventional vapor-compression refrigeration systems by utilizing natural working pairs. A common example is the silica gel–water cycle, in which silica gel serves as the adsorbent and water functions as the refrigerant.

In this study, a two-bed adsorption cooling system was experimentally investigated, featuring two alternately operating adsorption beds. Each half- cycle lasted approximately 195 min until the pressures stabilized and the temperature difference between the inlet and outlet of both beds reached zero. The average mass of desorbed water vapor was approximately 2.853 g per half-cycle, while the total heat supplied per half-cycle equaled 889.535 kJ, corresponding to a theoretical cooling capacity of 6.787 kJ and an estimated Energy Efficiency Ratio (EER) of 0.00763. In practical applications, this relatively low efficiency can be partially offset if the system is powered by low-cost or waste heat sources, including renewable thermal energy. The necessary measure is to better insulate the system so that the heat supplied to the system is equal to the heat removed from it. Future optimization strategies could also include the use of heat exchangers coated with silica-gel adsorbent to enhance heat and mass transfer, as well as the implementation of heat recovery and mass recovery between adsorption beds. These measures are expected to substantially improve both the cooling performance and overall efficiency of the system. Increasing the thermal contact between the heat exchanger surface and the adsorbent would also shorten the cycle duration, thereby improve the system's efficiency and increase the cooling capacity per unit time.

References

Australian Government. (2024). *Hydrofluorocarbon refrigerants – global warming potential values and safety classifications*. https://www.dcceew.gov.au/environment/protection/ozone/rac/global-warming-potential-values-hfc-refrigerants

Baheta, A. T., Hassan, S., Reduan, A. R. B., & Woldeyohannes, A. D. (2015). Performance investigation of transcritical carbon dioxide refrigeration cycle. *Procedia CIRP*, *26*, 482–485. https://doi.org/10.1016/j.procir.2015.02.084

Butrymowicz, D., Śmierciew, K., & Karwacki, J. (2014) Investigation of internal heat transfer in ejection refrigeration systems. *International Journal of Refrigeration*, *40*, 131–139. https://doi.org/10.1016/j.ijrefrig.2013.11.016

Darby, M. (2014, July 15). *Ozone layer treaty could tackle super polluting HFCs*. Climate home news. https://www.climatechangenews.com/2014/07/15/ozone-layer-treaty-could-tackle-super-polluting-hfcs/

Grzebielec, A. (2018). Długoterminowe magazynowanie energii w złożach sorpcyjnych [Long-term energy storage in absorption beds]. *Chłodnictwo i Klimatyzacja*, *53*(6), 11–13. https://doi.org/10.15199/8.2018.6.2

Grzebielec, A., & Szelągowski, A. (2020). Cold storage in sorption beds as effective solution enabling averaging of daily energy consumption. *Rynek Energii*, (4), 70–74.

Grzebielec, A. (2024). *Chłodnictwo i klimatyzacja. Perspektywiczne technologie* [Refrigeration and air conditioning. Prospective technologies]. PWN.

Hanif, S., Adiputra, S., Yaningsih, I., & Budiana, E. P. (2023). Adsorption characteristics of silica gel-water pairs in personal protection equipment. *Mekanika*: *Majalah Ilmiah Mekanika*, *22*(2), 50–58. https://doi.org/10.20961/mekanika.v22i2.71250

International Energy Agency. (2018). *Air conditioning use emerges as one of the key drivers of global electricity-demand growth*. https://www.iea.org/news/air-conditioning-use-emerges-as-one-of-the-key-drivers-of-global-electricity-demand-growth

Liu, Y. L., Wang, R. Z., & Xia, Z. Z. (2005). Experimental performance of a silica gel–water adsorption chiller. *Applied Thermal Engineering*, *25*(2–3), 359–375. https://doi.org/10.1016/j.applthermaleng.2004.06.012

Ludig, S., Jörß, W., & Liste, V. (2024). *Fluorinated greenhouse gases 2024* (ETC CM Report No. 2024-05). European Topic Centre on Climate Change Mitigation. https://www.dcceew.gov.au/environment/protection/ozone/rac/global-warming-potential-values-hfc-refrigerants

Najeh, G., Slimane, G., Souad, M., Riad, B., & Mohammed, E. G. (2016). Performance of silica gel-water solar adsorption cooling system. *Case Studies in Thermal Engineering*, *8*, 337–345. https://doi.org/10.1016/j.csite.2016.07.002

Sahu, D., Panda, J., Patnaik, A., & Mohapatra, A. K. (2026). Pro-gress in solid-vapor adsorption technology for eco-friendly refrigeration: Emphasizing metal halide sorbent. *Next Materials*, *11*, Article 101652. https://doi.org/10.1016/j.nxmate.2026.101652

The European Parliament & The Councli of the European Union. (2024). *Regulation* (*EU*) *2024/573 of the European Parliament and of the Council of 7 February 2024 on fluorinated greenhouse gases*, *amending Directive* (*EU*) *2019/1937 and repealing Regulation* (*EU*) *No 517/2014* (2024, February 7, No. 2024/573) https://eur-lex.europa.eu/legal-content/EN/TXT/?uri=CELEX%3A32024R0573&qid=1747845254004

Thu, K., Chakraborty, A., Saha, B. B., & Ng, K. C. (2013). Thermo-physical properties of silica gel for adsorption desalination cycle. *Applied Thermal Engineering*, *50*(2), 1596–1602. https://doi.org/10.1016/j.applthermaleng.2011.09.038

Szelągowski, A., & Chwieduk, D. (2025). *Badanie eksperymentalne wpływu wielkości ziaren żelu krzemionokowego na zdolność magazynowa ciepła z zastosowaniem powłok adsorpcyjnych* [An experimental study of the effect of silica gel particle size on heat storage capacity using adsorption coatings]. In M. Piasecka (Ed.), *Rozwiązania w Wymianie Ciepła i Masy*. *Wyzwania i Perspektywy*.